Essential requirement for two-pore channel 1 in NAADP-mediated calcium signaling

Eugen Brailoiu,[1] Dev Churamani,[2] Xinjiang Cai,[3] Michael G. Schrlau,[4] G. Cristina Brailoiu,[1] Xin Gao,[1] Robert Hooper,[2] Michael J. Boulware,[5] Nae J. Dun,[1] Jonathan S. Marchant,[5] and Sandip Patel[2]

[1]Department of Pharmacology, Temple University School of Medicine, Philadelphia, PA 19140
[2]Department of Cell and Developmental Biology, University College London, London WC1E 6BT, England, UK
[3]Division of Cardiology, Department of Medicine, Duke University Medical Center, Durham, NC 27710
[4]Department of Mechanical Engineering and Applied Mechanics, University of Pennsylvania, Philadelphia, PA 19104
[5]Department of Pharmacology, University of Minnesota Medical School, Minneapolis, MN 55455

Nicotinic acid adenine dinucleotide phosphate (NAADP) is a widespread and potent calcium-mobilizing messenger that is highly unusual in activating calcium channels located on acidic stores. However, the molecular identity of the target protein is unclear. In this study, we show that the previously uncharacterized human two-pore channels (TPC1 and TPC2) are endolysosomal proteins, that NAADP-mediated calcium signals are enhanced by overexpression of TPC1 and attenuated after knockdown of TPC1, and that mutation of a single highly conserved residue within a putative pore region abrogated calcium release by NAADP. Thus, TPC1 is critical for NAADP action and is likely the long sought after target channel for NAADP.

Introduction

Release of stored calcium by calcium-mobilizing messengers such as inositol trisphosphate, cyclic ADP-ribose, and nicotinic acid adenine dinucleotide phosphate (NAADP) is a ubiquitous mechanism for effecting changes in cytosolic calcium (Berridge et al., 2000). Inositol trisphosphate receptors (Foskett et al., 2007) and ryanodine receptors (Fill and Copello, 2002) are well-defined calcium channels located on ER calcium stores that open in response to receptor-mediated generation of inositol trisphosphate and cyclic ADP-ribose, respectively (Berridge et al., 2000). In contrast, the molecular basis for calcium release by NAADP, the most contemporary of the calcium-mobilizing messengers, is not established (Lee, 2005; Guse and Lee, 2008).

Although NAADP appears to directly release calcium from the ER in some cells (Gerasimenko et al., 2003; Steen et al., 2007), the bulk of the current evidence suggests that NAADP is an atypical messenger activating a novel channel located not on the ER but instead on acidic calcium stores (Berridge et al., 2002; Churchill et al., 2002; Mitchell et al., 2003; Kinnear et al., 2004; Yamasaki et al., 2004; Brailoiu et al., 2005, 2006; Zhang et al., 2006; Kim et al., 2008; Gambara et al., 2008). Despite such segregation, the activation of NAADP-sensitive calcium channels invariably triggers further calcium release via inositol trisphosphate/ryanodine receptors through the process of calcium-induced calcium release (Cancela et al., 1999). Consequently, NAADP is a key determinant of complex calcium signals that result upon physiological stimulation in response to certain agonists (Guse and Lee, 2008). Indeed, so-called "chatter" (Patel et al., 2001) between NAADP, inositol trisphosphate, and cyclic ADP-ribose has been implicated in several calcium-dependent events, including fertilization (Albrieux et al., 1998; Churchill et al., 2003), glucose sensing (Masgrau et al., 2003; Kim et al., 2008), neuronal growth (Brailoiu et al., 2005), and differentiation (Brailoiu et al., 2006). However, the molecular identity of the target channel for NAADP is not clear. Although both ryanodine receptors (Mojzisova et al., 2001; Hohenegger et al., 2002) and the lysosomal ion channel TRPML1 (Zhang and Li, 2007) have been proposed as candidates, direct contradictory evidence has also been obtained (Copello et al., 2001; Dong et al., 2008). In addition, NAADP may activate TRPM2 channels on the plasma membrane (Beck et al., 2006) to mediate calcium influx. The nature of the NAADP-sensitive channel is therefore equivocal and hotly debated (Galione and Petersen, 2005).

Correspondence to Sandip Patel: patel.s@ucl.ac.uk

Abbreviations used in this paper: HEK, human embryonic kidney; mRFP, monomeric RFP; NAADP, nicotinic acid adenine dinucleotide phosphate; shRNA, short hairpin RNA; TPC, two-pore channel.

© 2009 Brailoiu et al. This article is distributed under the terms of an Attribution–Noncommercial–Share Alike–No Mirror Sites license for the first six months after the publication date (see http://www.jcb.org/misc/terms.shtml). After six months it is available under a Creative Commons License (Attribution–Noncommercial–Share Alike 3.0 Unported license, as described at http://creativecommons.org/licenses/by-nc-sa/3.0/).

The Rockefeller University Press $30.00
J. Cell Biol. Vol. 186 No. 2 201–209
www.jcb.org/cgi/doi/10.1083/jcb.200904073

THE JOURNAL OF CELL BIOLOGY

Downloaded from http://rupress.org/jcb/article-pdf/186/2/201/1892586/jcb_200904073.pdf by guest on 08 February 2026

The two-pore channel (TPC) has recently emerged as a novel intracellular calcium release channel in plants (Peiter et al., 2005). TPCs have a domain structure similar to one-half of voltage-sensitive Ca^{2+} channels; i.e., they are composed of two repeats of six trans-membrane helices each encompassing a putative pore (Peiter et al., 2005). In *Arabidopsis thaliana*, TPC is likely the molecular correlate of the well-characterized slow vacuolar current and has been implicated in several Ca^{2+}-dependent processes (Pottosin and Schonknecht, 2007). Surprisingly, apart from the initial cloning and characterization of rat TPC1 (Ishibashi et al., 2000), scant information is currently available regarding TPCs in animals.

In this study, we show that animal TPCs constitute a ubiquitous and expanded family of novel endolysosomal proteins. Using a combined overexpression and knockdown approach, we demonstrate that TPC1 dictates cellular sensitivity to NAADP. In addition, we identify a highly conserved residue in the putative pore region of TPCs that is critical for function. Our data suggest that TPCs are likely the elusive NAADP receptors.

Results and discussion

An expanded family of TPC genes in animals

TPCs are almost completely uncharacterized in animals. Comparative genomic analysis reveals that the TPC gene is widespread in the animal kingdom and has undergone multiplication with most species possessing either two (human and rat) or three (sea urchin) TPC genes (Fig. 1 A and Table S1). These genes are predicted to encode for proteins that display ~35% sequence similarity (Table S2). Duplication of the TPC gene likely began early during animal evolution given the presence of multiple TPC genes in the sea anemone (*Nematostella vectensis*; Fig. 1 A), a member of the Cnidarian phylum considered the oldest of the eumetazoan lineage. Indeed, multiple TPC genes are also evident in the choanoflagellate *Monosiga brevicollis*, which is a close unicellular relative of animals (Fig. 1 A). Intriguingly, a single copy of the TPC gene is present in the protists *Thalassiosira pseudonana* (marine phytoplankton) and *Phytophthora ramorum* (sudden oak death pathogen; Fig. 1 A), suggesting that TPCs are ancient proteins that likely originated in the common ancestor of animals and plants. During the course of metazoan evolution, we note lineage-specific gene loss. This is most striking in mammals, where three genes are present in some species such as dog, whereas only two are present in other species such as human and rat (Fig. 1 A and Table S1). Semiquantitative RT-PCR analysis demonstrated the presence of transcripts for all three TPC isoforms in sea urchin eggs in which the effects of NAADP were first described (Lee and Aarhus, 1995), although levels of TPC3 were low compared with prism-stage embryos (Fig. 1 B). TPC1 and TPC2 transcripts were also detectable in rat PC12 and human SKBR3 cells (Fig. 1 B), which are cell lines that have both been shown to respond to NAADP (Brailoiu et al., 2006; Schrlau et al., 2008). Quantitative PCR indicated that TPC1 was the major isoform expressed in sea urchin eggs, PC12, and SKBR3 cells (Fig. 1 C). Therefore, TPCs comprise a ubiquitous family of novel uncharacterized ion channels in animals.

Human TPCs are intracellular proteins targeted to the endolysosomal system

The location of *A. thaliana* TPC to the vacuole (Peiter et al., 2005), the functional equivalent of the animal endolysosomal system, raises the possibility that animal TPCs may be a novel class of endolysosomal ion channels. To test this hypothesis, we expressed monomeric RFP (mRFP)–tagged human TPC1 and TPC2 in *Xenopus laevis* oocytes. Confocal microscopy of live oocytes indicated that both isoforms were clearly intracellular, as shown by lack of fluorescence at the level of the plasma membrane (Fig. 2, A and B). High resolution imaging revealed targeting to a population of discrete vesicles (Fig. 2, C and D). A vesicular location was also found for TPC1 and TPC2 heterologously expressed in human SKBR3 cells (Fig. 2, E and F). Such an intracellular location for TPCs may in part explain why in a previous study, no membrane currents were recorded in *X. laevis* oocytes and CHO cells overexpressing rat TPC1 (Ishibashi et al., 2000). To determine the identity of the vesicles, TPC1 and TPC2 were coexpressed with various organelle markers. We found significant colocalization of TPC1 with markers for both lysosomes/late endosomes (LAMP1) and endosomes (endo-GFP) but not the ER (DsRed2-KDEL; Fig. 2 E). Heterologously expressed TPC2 colocalized with LAMP-1 only (Fig. 2 F). Intriguingly, a recent genetic screen has identified coding variants of human TPC2 that are associated with hair pigmentation (Sulem et al., 2008). That pigment synthesis occurs in melanosomes; a lysosome-related organelle is entirely consistent with the localization of human TPC2 to the lysosome reported in this study. Collectively, these data demonstrate that human TPCs are a new family of intracellular proteins targeted to the endolysosomal system.

Overexpression and knockdown of TPC1 dictates NAADP sensitivity

Given the location of TPCs to acidic vesicles, we next tested whether TPCs are NAADP-sensitive calcium channels by examining the effect of overexpressing TPC1 on NAADP-mediated calcium signals. We used SKBR3 cells in which we have previously characterized the effects of NAADP (Schrlau et al., 2008). Microinjection of buffer had little effect on cytosolic calcium levels of mock-transfected cells and cells overexpressing TPC1 (Fig. 3, A and D). Microinjection of a subthreshold concentration of NAADP (10 nM pipette concentration) was also largely ineffective in elevating cytosolic calcium levels in mock-transfected cells (Fig. 3, B and D). In contrast, robust responses to NAADP injection were observed in cells overexpressing either TPC1 mRFP (Fig. 3, B and D; and Fig. S1) or TPC2 GFP (not depicted). This pronounced sensitization is consistent with TPCs functioning as NAADP-sensitive calcium channels. Indeed, overexpression of TPCs in *X. laevis* oocytes, which are normally insensitive to NAADP (Marchant and Parker, 2001), conferred NAADP sensitivity, although the NAADP-mediated calcium signals were smaller in magnitude and slower to peak than calcium signals evoked by inositol trisphosphate (unpublished data).

We have previously shown that endogenous NAADP-mediated responses in SKBR3 cells (which are readily evoked

Downloaded from http://rupress.org/jcb/article-pdf/186/2/201/1892586/jcb_200904073.pdf by guest on 08 February 2026

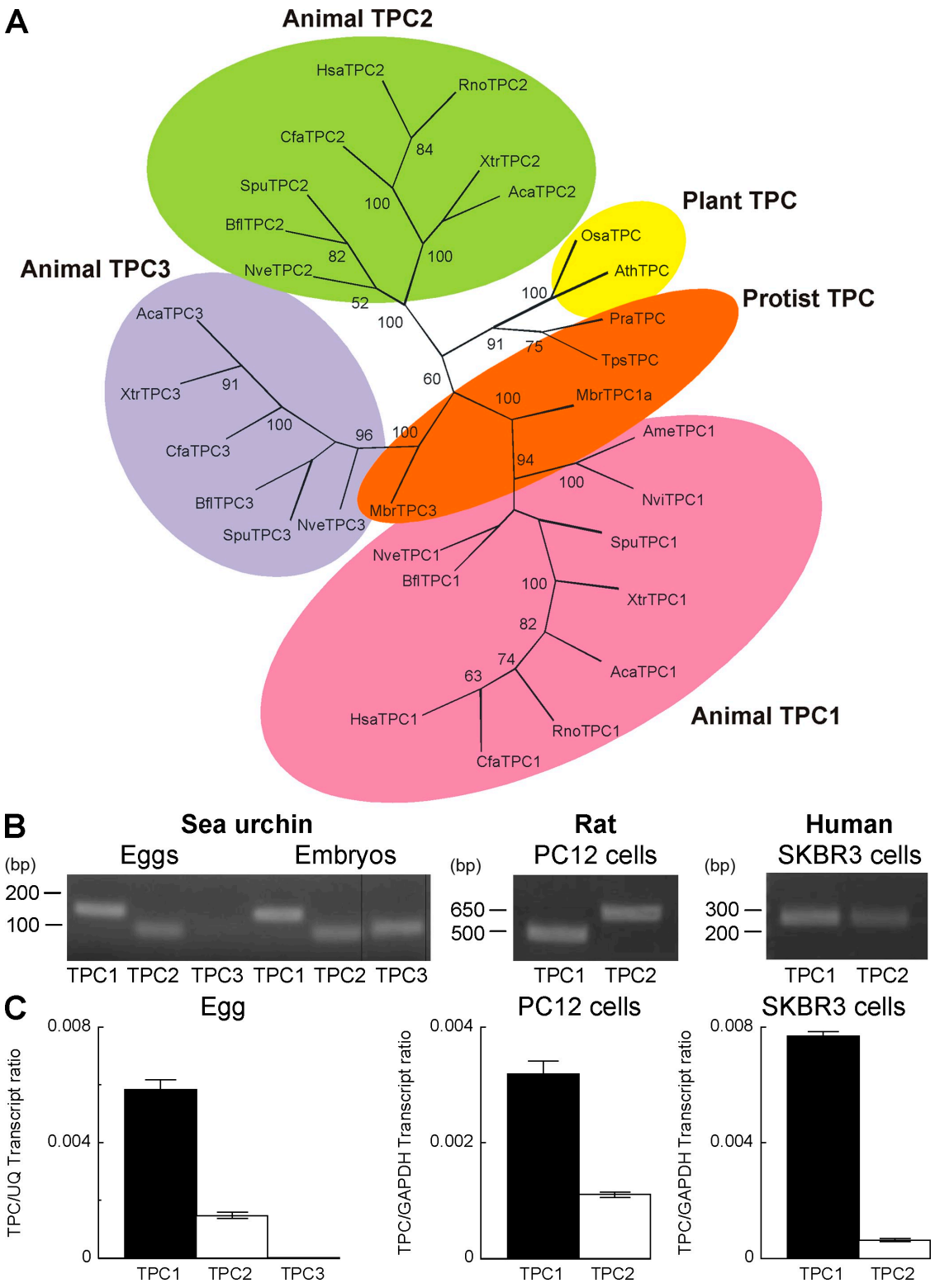

Figure 1. **An expanded family of TPC genes in animals.** (A) Maximum likelihood tree constructed using the conserved regions of TPC sequences from the representative organisms listed in Table S1. Shading highlights TPC isoforms in plants, protists, and animals, with the latter subdivided into three distinct groupings. Bootstrap values >50 are shown at the branches. (B) End point RT-PCR analysis showing expression of transcripts for TPC isoforms in the indicated cell type/embryo (prism stage). The expected sizes of the amplicons were 152 (SpuTPC1), 93 (SpuTPC2), 107 (SpuTPC3), 473 (RnoTPC1), 575 (RnoTPC2), 250 (HsaTPC1), and 250 bp (HsaTPC2). Black lines indicate that intervening lanes have been spliced out. (C) Quantitative RT-PCR of TPC isoforms. Data were normalized to the expression level of the indicated housekeeping gene. Error bars indicate SEM.

Downloaded from http://rupress.org/jcb/article-pdf/186/2/201/1892586/jcb_200904073.pdf by guest on 08 February 2026

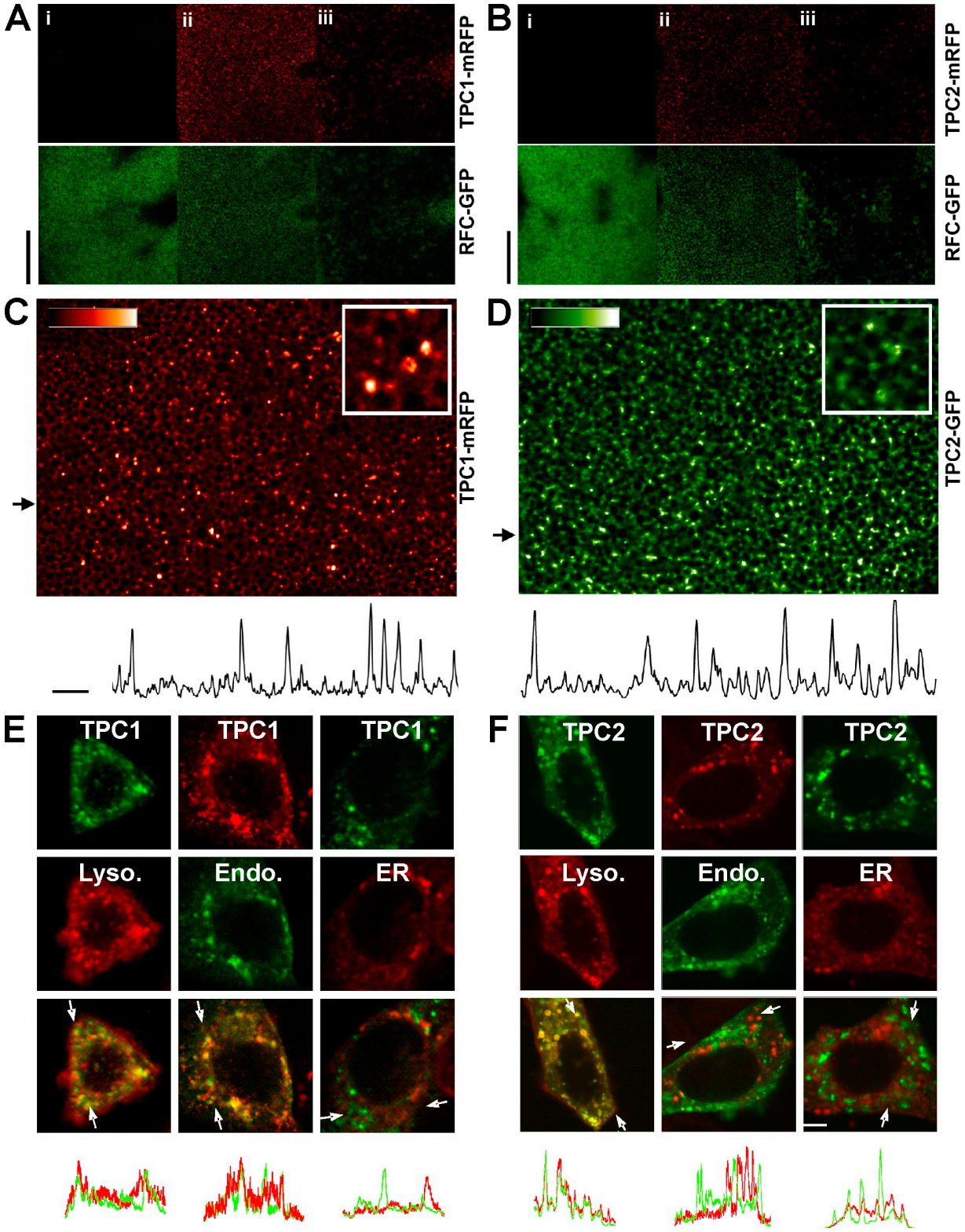

Figure 2. **TPCs are intracellular proteins targeted to the endolysosomal system.** (A and B) Confocal images of *X. laevis* oocytes coexpressing a plasma membrane marker (human reduced folate carrier [RFC]–GFP; green) and either TPC1-mRFP (A) or TPC2-mRFP (B). Images were taken at the level of the plasma membrane (i), cortical ER (ii), and subcortical ER (iii). Bars, 30 µm. (C and D) Higher magnification images of TPC1-mRFP (C) and TPC2-GFP expression (D). Insets show a digitally zoomed region. Plots of fluorescence intensity from regions indicated by the arrows are shown below. Bars, 10 µm. (E and F) Confocal images of SKBR3 cells coexpressing TPC1 (E) or TPC2 (F) tagged with either mRFP or GFP (top row) and organelle markers (middle row) for lysosomes (Lyso)/late endosomes (LAMP1-mRFP; left column), early and late endosomes (endo-GFP; middle column), or the ER (DsRed2-KDEL; right column). Overlays of the images are shown in the bottom rows. Intensity plots of green and red fluorescence across the regions delimited by the arrows in the overlay images are shown below. Bar, 5 µm.

Downloaded from http://rupress.org/jcb/article-pdf/186/2/201/1892586/jcb_200904073.pdf by guest on 08 February 2026

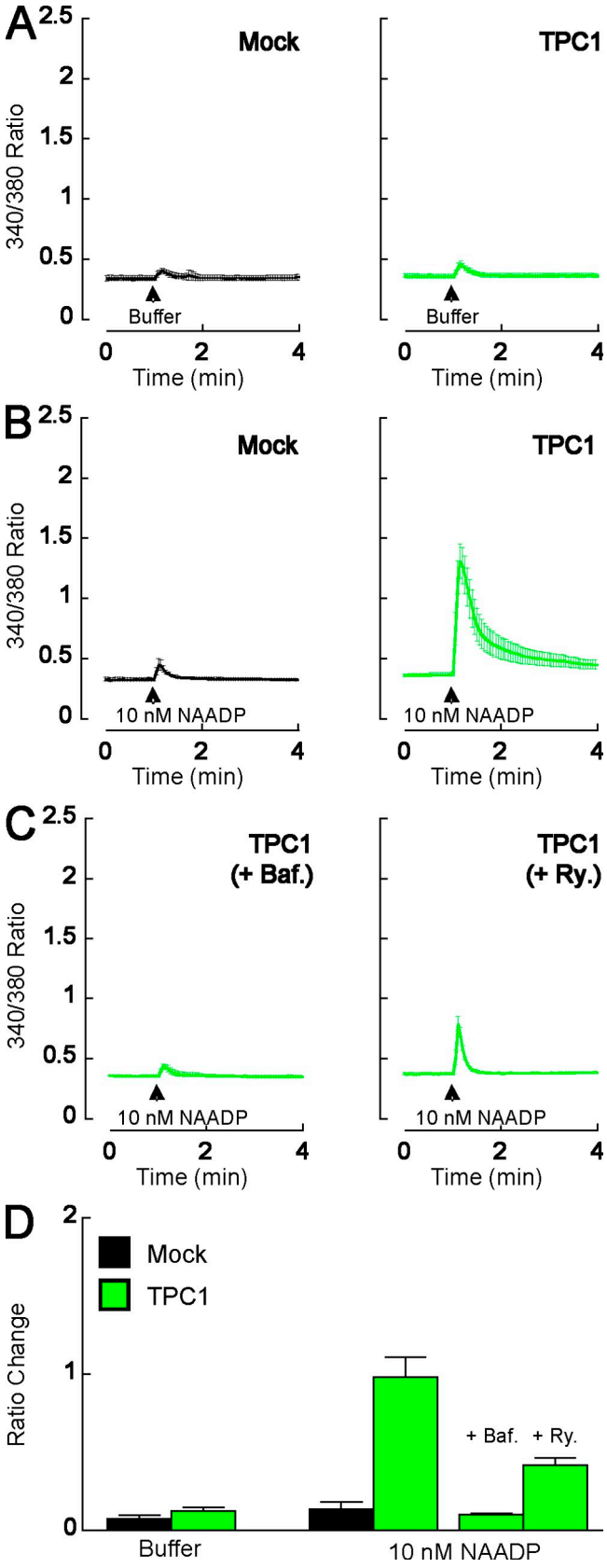

Figure 3. **Overexpression of TPC1 enhances NAADP-mediated calcium signals.** (A–C) Cytosolic calcium responses of individual fura-2–loaded SKBR3 cells microinjected with either buffer (A) or 10 nM NAADP (B and C). Cells were from mock-transfected cultures (black) or cultures expressing TPC1 mRFP (green). In C, cells were pretreated with 1 µM bafilomycin A1 (Baf) for 60 min or 10 µM ryanodine (Ry) for 15 min as indicated. Data are expressed as mean fluorescence ratios from 4–11 cells. (D) Pooled data quantifying the magnitude of the ratio changes under the various experimental conditions. Error bars indicate SEM.

at higher concentrations of NAADP; Fig. 4) are inhibited by blockade of either V-type ATPases with bafilomycin or ryanodine receptors with ryanodine (Schrlau et al., 2008). The former likely prevents proton-dependent calcium uptake into acidic organelles (Churchill et al., 2002). These data support the hypothesis that in response to NAADP, calcium signals derive from acidic stores and are amplified by ryanodine receptors. To determine the source of NAADP-mediated calcium signals in cells overexpressing TPC1, we examined the effects of 1 µM bafilomycin and 10 µM ryanodine on NAADP responses. As shown in Fig. 3 (C and D), calcium signals in response to NAADP were substantially reduced by both inhibitors. Thus, the pharmacology of endogenous NAADP responses and responses upon overexpression of TPC1 are similar if not identical, providing additional evidence that TPC1 is a NAADP-sensitive calcium channel. NED19, a newly described NAADP antagonist (Naylor et al., 2009), could not be used in this cell type because when added alone at a concentration of 100 µM, it evoked a cytosolic calcium increase (unpublished data).

To further investigate the role of TPC1 in NAADP-mediated calcium signaling, we determined the contribution of endogenous TPC1 in SKBR3 cells to NAADP responses. To achieve this, we inhibited expression of TPC1 using RNA interference. In mock-transfected cells and cells expressing a control short hairpin RNA (shRNA) together with a GFP reporter, injection of 10 µM NAADP mediated a robust calcium signal (Fig. 4 A). Both the basal and peak fluorescence ratios were similar in the two conditions, indicating that GFP did not interfere with the calcium measurements. In marked contrast, cells expressing a shRNA that selectively suppresses expression of TPC1 (Fig. S2) were substantially less sensitive to NAADP (Fig. 4 A). These data, summarized in Fig. 4 B, provide strong evidence that TPC1 mediates endogenous NAADP responses in SKBR3 cells.

Cytosolic calcium responses to a submaximal concentration of cyclic ADP-ribose (50 nM pipette concentration), which activates ryanodine receptors through calcium-induced calcium release (Berridge et al., 2000), were unaffected by either overexpression or knockdown of TPC1 (Fig. S3, A and B), highlighting the specificity of the manipulations. Collectively, the data in Figs. 3 and 4 show that NAADP sensitivity is critically dependent on expression of TPC1. What role other TPC isoforms play remains to be established, although we find that TPC1 appears to be the major isoform expressed in several NAADP-sensitive cells (Fig. 1 C).

Mutation of a single residue in the putative pore region inactivates TPC1

An alignment of the amino acid sequences of putative pore regions of TPCs from several animals reveals two residues that are conserved in both pores and across species (Fig. 5 A, asterisks). One of these residues (leucine 273 in human TPC1) is in the putative helix of the pore-forming region (Fig. 5 A). Mutation of this residue to a

Downloaded from http://rupress.org/jcb/article-pdf/186/2/201/1892586/jcb_200904073.pdf by guest on 08 February 2026

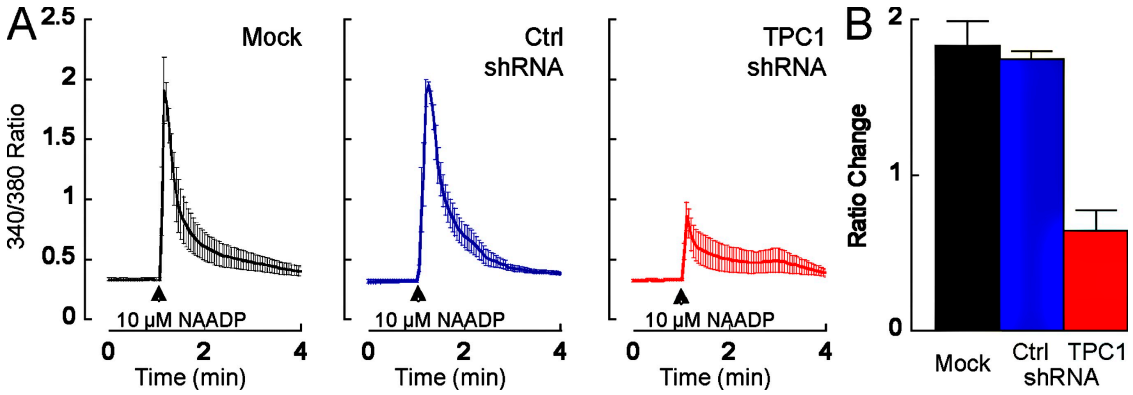

Figure 4. **Knockdown of TPC1 reduces NAADP-mediated calcium signals.** (A) Cytosolic calcium responses of individual fura-2–loaded SKBR3 cells microinjected with 10 μM NAADP. Cells were from mock-transfected cultures (black) or cultures expressing either a control (Ctrl) shRNA (blue) or an shRNA-targeting TPC1 (red). (B) Pooled data quantifying the magnitude of the ratio changes under the various experimental conditions. Error bars indicate SEM.

helix-breaking proline residue abolished the potentiating effects of TPC1 overexpression on NAADP-mediated calcium signals (Fig. 5 B). The lack of response was not caused by mistargeting of TPC1 L273P because the mutant protein colocalized with wild-type TPC1 (Fig. S3 C). We also found that calcium signals, in response to higher concentrations of NAADP, were significantly reduced in cells overexpressing TPC1 L273P (Fig. 5 C), suggesting that this mutant acts in a dominant-negative manner. These data, summarized in Fig. 5 D, further confirm the specificity of the effect of overexpressing wild-type TPC1 on NAADP-mediated calcium signals, provide additional evidence that endogenous NAADP responses require TPCs, and show that TPC function is likely dependent on ion channel activity. Most ion channel pores are formed through assembly of at least three pore-forming subunits. Given the sequence similarity between TPCs and voltage-sensitive calcium and sodium channels (Ishibashi et al., 2000), which are composed of four repeats, it is tempting to speculate that TPCs are dimeric. Thus, the observed dominant-negative action of TPC1 L273P may result in oligomerization of the mutant with endogenous channels and should prove a powerful tool in future studies to inhibit NAADP signaling.

In summary, we identify animal TPCs as a new and ubiquitous class of endolysosomal ion channels. By combining overexpression, knockdown, and mutagenesis, we show that TPC1 is critically involved in NAADP action. Our data provide molecular evidence, which has been lacking until now, to support the hypothesis that NAADP targets novel channels situated on acidic calcium stores. Indeed, the results presented in this study are consistent with a very recent study that also provides evidence that TPCs are endolysosomal channels targeted by NAADP (Calcraft et al., 2009). We conclude that TPCs are an essential component of the molecular machinery underlying calcium signals in response to NAADP and are likely the direct target for this highly potent calcium-mobilizing messenger.

Materials and methods

Phylogenetics

BlastP and TBlastN searches (Altschul et al., 1997) were performed against the genomic and protein databases of the National Center for Biotechnology Information (http://www.ncbi.nlm.nih.gov/blast/) and the Department of Energy Joint Genome Institute (http://genome.jgi-psf.org/) using protein sequences of human and sea urchin (*Stronglyocentrotus purpuratus*) TPCs. Sequence datasets were retrieved for sequence alignment followed by manual editing and phylogenetic analysis, essentially as described previously (Cai and Zhang, 2006; Cai, 2007).

RT-PCR

Total RNA was extracted using the RNeasy mini kit (QIAGEN) according to the manufacturer's instructions. cDNA was prepared using a reverse transcription system (ImProm-II; Promega) with oligo dT primers. Oligonucleotide primers designed to the nucleotide sequences of sea urchin TPC1-3 (unpublished data), rat TPC1 (GenBank/EMBL/DDBJ accession no. NM_139332), rat TPC2 (GenBank/EMBL/DDBJ accession no. NM_001107566), human TPC1 (GenBank/EMBL/DDBJ accession no. BC150203), and human TPC2 (GenBank/EMBL/DDBJ accession no. BC063008) are listed in Table S3. For end point PCRs, samples were denatured for 2 min at 94°C followed by 35 cycles of denaturation (30 s at 94°C), annealing (30 s at 50°C), and extension (1 min at 68°C) using DNA polymerase (Platinum Taq High Fidelity; Invitrogen). For quantitative PCR, samples were denatured for 2 min at 94°C followed by 40 cycles of denaturation (15 s at 94°C), annealing (30 s at 60°C), and extension (30 s at 72°C) using SYBR Green JumpStart Taq Ready-Mix (Sigma-Aldrich). Expression levels were normalized to the expression of ubiquitin (for sea urchin samples) and glyceraldehyde 3-phosphate dehydrogenase (for rat and human samples) after parallel amplification using the indicated oligonucleotide primers (Table S3).

Plasmid constructs

pCS2+ vectors into which the coding sequences for either mRFP or EGFP had been inserted at the XhoI and XbaI sites were provided by M. Tada (University College London, London, England, UK). The full-length coding sequence for human TPC1 and TPC2 were amplified by PCR using IMAGE clones 40148827 (GenBank/EMBL/DDBJ accession no. BC150203) and 5214862 (GenBank/EMBL/DDBJ accession no. BC063008), respectively, as templates. TPC1 was inserted in frame into pCS2+ mRFP or pCS2+ GFP at the ClaI and EcoRI sites to generate plasmids encoding for TPC1 tagged at the C terminus with the fluorescent reporter molecule. TPC2 was inserted at the EcoRI and XhoI sites. A construct in which leucine 273 of mRFP-tagged TPC1 was substituted for proline (TPC1 L273P) was generated by sequence overlap extension (Horton et al., 1990) using mutagenic (forward,5′-TGGAGAACAGCATCGTCAGTCCGTTTGTCCTTCTGACCAC-AGC-3′; reverse, 5′-CGGACTGACGATGCTGTTCTCCA-3′) and outer (forward, 5′-ATTTTCCTGGTGGACTGTCG-3′; reverse, 5′-AGGAAGGCGA-ACACTGTCAC-3′) primer pairs to generate a cassette that was subsequently cloned into pCS2+ TPC1 mRFP at the BglII and BsPE1 sites. For cellular expression of shRNA, complementary oligonucleotides corresponding to a TPC1 target sequence (5′-CGAGCTGTATTTCATCATGAA-3′) or control sequence (5′-AATTCTCCGAACGTGTCACGT-3′) were synthesized and cloned directly into the pSUPER + GFP vector (Oligoengine) according to the manufacturer's instructions. This bicistronic vector allows coexpression of both GFP and shRNA in the same cell. The control vector was provided by R. Holic and S. Cockcroft (University College London). siRNA duplexes corresponding to the TPC1 target sequence were purchased from QIAGEN. The fidelity of all constructs was verified by direct sequencing.

Downloaded from http://rupress.org/jcb/article-pdf/186/2/201/1892586/jcb_200904073.pdf by guest on 08 February 2026

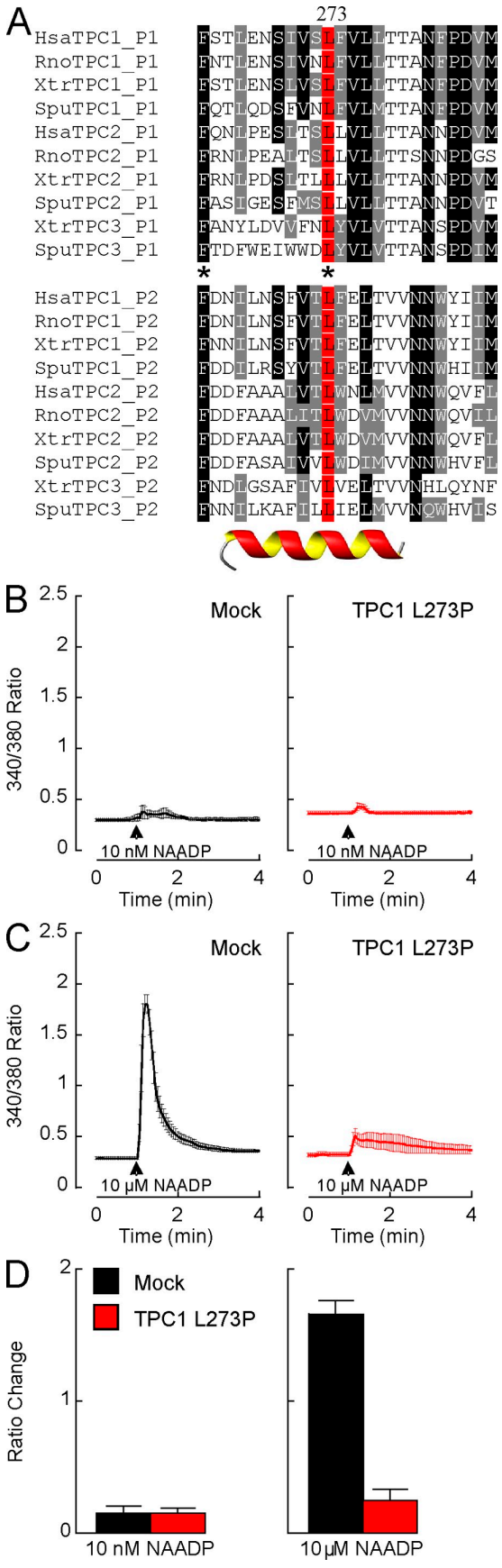

Figure 5. **Mutation of a single residue in the putative pore region inactivates TPC1.** (A) Multiple sequence alignment of the two putative pore regions (P1 and P2) of several animal TPCs. Asterisks highlight residues conserved in both pores of all isoforms from different species. Predicted helical region is outlined by the cartoon. (B and C) Cytosolic calcium responses of individual fura-2–loaded SKBR3 cells microinjected with either 10 nM (B) or 10 µM (C) NAADP. Cells were from mock-transfected cultures or cultures expressing TPC1 mutated in the putative pore region (TPC1 L273P). (D) Pooled data quantifying the magnitude of cytosolic changes under the various experimental conditions are shown. Error bars indicate SEM.

Cell culture

Gametes from *S. purpuratus* were obtained by intracoelemic injection of 0.5 M KCl and collected either dry (sperm) or into filtered sea water (eggs). Dejellied eggs (5% vol/vol) were fertilized by addition of concentrated sperm, washed three times, and maintained (0.5% vol/vol) with gentle stirring at 16°C in filtered sea water supplemented with 50 µg/ml streptomycin. Prism-stage embryos were collected 46 h after fertilization. Stage VI *X. laevis* oocytes were collected from female *X. laevis* and maintained in modified Barth's saline supplemented with 25 µg/ml gentamicin (Sigma-Aldrich). Rat adrenal pheochromocytoma (PC12) cells were maintained in RPMI 1640 medium supplemented with 5% fetal bovine serum and 10% heat-inactivated horse serum. SKBR3 human breast carcinoma cells were maintained in McCoy's 5A modified media and 10% fetal bovine serum. Human embryonic kidney (HEK) cells were maintained in DME and 10% (vol/vol) fetal bovine serum. All cell lines were cultured in the presence of 100 U/ml penicillin and 100 µg/ml streptomycin at 37°C in a humidified atmosphere of 95% air and 5% COB_{2B}.

Oocyte expression

X. laevis oocytes were defolliculated by incubation with 2 mg/ml collagenase type 1A (Sigma-Aldrich) in modified Barth's saline for 2 h with agitation. cDNA for mRFP- or GFP-tagged TPC1 and TPC2 and GFP-tagged human reduced folate carrier (Subramanian et al., 2001) was microinjected (~8 ng plasmid) directly into the nucleus of the oocyte, and cells were imaged 2 d after injection.

Transfection of SKBR3 and HEK cells

Cells were seeded onto glass coverslips coated with 20 µg/ml poly-L-lysine and transiently transfected with plasmid DNA using either transfection reagent (Lipofectamine2000; Invitrogen) or DharmaFECT (Thermo Fisher Scientific) according to the manufacturers' instructions. Cells were used 1–3 d after transfection. For localization experiments, cells were cotransfected with mRFP- or GFP-tagged TPC1 and TPC2 together with LAMP1-mRFP (Sherer et al., 2003), pEGFP-endo (Clontech Laboratories, Inc.), or pDsRed2-ER (Clontech Laboratories, Inc.) and fixed before confocal microscopy.

Confocal microscopy

Images of live oocytes bathed in Ringer's solution were captured using a confocal scanner (MRC1024; Bio-Rad Laboratories) attached to a microscope (AX70; Olympus) equipped with 40× NA 1.3 and 60× NA 1.42 oil immersion objective lenses. Images were colored using Interactive Data Language software (ITT Visual Information Solutions). Images of fixed SKBR3 and HEK cells were captured using a confocal scanner (LSM 510; Carl Zeiss, Inc.) attached to a microscope (Axiovert 200M; Carl Zeiss, Inc.) equipped with a 10× 0.3 NA Plan Neofluar objective, a 40× NA 1.3 Plan Neofluar oil immersion objective, and a 63× 1.4 NA Plan Apochromat oil immersion objective. The respective excitation and emission wavelengths were 488 and 505–550 nm for GFP and 543 and 560–615 nm for DsRed2/mRFP.

Microinjection of SKBR3 cells

Injections were performed using Femtotips I, InjectMan N12, and Femtojet systems (Eppendorf). Pipettes were back filled with an intracellular solution composed of 110 mM KCl, 10 mM NaCl, and 20 mM Hepes, pH 7.2, and supplemented with or without 10 nM or 10 µM NAADP or 50 nM cyclic ADP-ribose. The injection time was 0.5 s at 75 hPa with a compensation pressure of 25 hPa. Transfected cells were identified by capturing fluorescence of the reporter molecule (mRFP for the TPC1 constructs or GFP for TPC2 and the shRNA constructs). Only cells that maintained a resting basal fura-2 fluorescence ratio (see following paragraph) of <0.5 and that expressed similar levels of the reporter were selected for injection.

Downloaded from http://rupress.org/jcb/article-pdf/186/2/201/1892586/jcb_200904073.pdf by guest on 08 February 2026

Calcium imaging

Cells were incubated with 5 µM fura-2 AM (Invitrogen) in Hanks' balanced salt solution at room temperature for 45 min in the dark, washed three times with dye-free buffer, and incubated for another 45 min to allow for deesterification of the dye. Coverslips were subsequently mounted in a custom-designed bath on the stage of an inverted microscope (Eclipse TE 2000-U; Nikon) equipped with a 40× NA 1.3 oil immersion objective and a charge-coupled device camera (Roper Scientific; Optical Apparatus Co.). Cells were superfused with Hanks' balanced salt solution at a flow rate of 0.5 ml/min. Fura-2 fluorescence (510-nm emission), after alternate excitation at 340 and 380 nm, was acquired at a frequency of 0.33 Hz. Captured images were analyzed using MetaFluor software (MDS Analytical Technologies). Autofluorescence was negligible.

Online supplemental material

Fig. S1 shows the variation in single-cell responses to NAADP injection, Fig. S2 validates TPC1 siRNA, and Fig. S3 shows that overexpression or knockdown of TPC1 does not affect cyclic ADP-ribose–mediated calcium signals and that TPC1 L273P colocalizes with wild-type TPC1. Table S1 lists the protein sequences used for phylogenetic analyses, Table S2 summarizes amino acid sequence identity and similarity between members of the TPC family, and Table S3 lists the sequences of oligonucleotide primers used in this study. Online supplemental material is available at http://www.jcb.org/cgi/content/full/jcb.200904073/DC1.

We thank Charles Cox, Leslie Dale, Caroline Dalton, George Dickinson, Annette Dolphin, Caroline Hew, Hina Quayum, Latha Ramakrishnan, Mary Rahman, and Revathi Ragendran for help with pilot experiments and Shamshad Cockcroft, Roman Holic, Chi Li, and Victor D. Vacquier for advice and provision of reagents.

This work was supported by the Biotechnology and Biological Sciences Research Council (grants BB/D018110/1 and BB/G013721/1 to S. Patel), the Wellcome Trust (grant VS/07/UCL/A7 to S. Patel), the National Institutes of Health (grants HL90804 to E. Brailoiu, GM08879 to J.S. Marchant, and NS18710 and HL51314 to N.J. Dun), and the American Heart Association (Fellowship Award 0625403U to X. Cai).

Submitted: 14 April 2009
Accepted: 25 June 2009

References

Albrieux, M., H.C. Lee, and M. Villaz. 1998. Calcium signaling by cyclic ADP-ribose, NAADP, and inositol trisphosphate are involved in distinct functions in ascidian oocytes. *J. Biol. Chem.* 273:14566–14574.

Altschul, S.F., T.L. Madden, A.A. Schaffer, J. Zhang, Z. Zhang, W. Miller, and D.J. Lipman. 1997. Gapped BLAST and PSI-BLAST: a new generation of protein database search programs. *Nucleic Acids Res.* 25:3389–3402.

Beck, A., M. Kolisek, L.A. Bagley, A. Fleig, and R. Penner. 2006. Nicotinic acid adenine dinucleotide phosphate and cyclic ADP-ribose regulate TRPM2 channels in T lymphocytes. *FASEB J.* 20:962–964.

Berridge, G., G. Dickinson, J. Parrington, A. Galione, and S. Patel. 2002. Solubilization of receptors for the novel Ca^{2+}-mobilizing messenger, nicotinic acid adenine dinucleotide phosphate. *J. Biol. Chem.* 277:43717–43723.

Berridge, M.J., P. Lipp, and M.D. Bootman. 2000. The versatility and universality of calcium signalling. *Nat. Rev. Mol. Cell Biol.* 1:11–21.

Brailoiu, E., J.L. Hoard, C.M. Filipeanu, G.C. Brailoiu, S.L. Dun, S. Patel, and N.J. Dun. 2005. NAADP potentiates neurite outgrowth. *J. Biol. Chem.* 280:5646–5650.

Brailoiu, E., D. Churamani, V. Pandey, G.C. Brailoiu, F. Tuluc, S. Patel, and N.J. Dun. 2006. Messenger-specific role for NAADP in neuronal differentiation. *J. Biol. Chem.* 281:15923–15928.

Cai, X. 2007. Molecular evolution and functional divergence of the Ca2+ sensor protein in store-operated Ca2+ entry: stromal interaction molecule. *PLoS One.* 2:e609.

Cai, X., and Y. Zhang. 2006. Molecular evolution of the ankyrin gene family. *Mol. Biol. Evol.* 23:550–558.

Calcraft, P.J., M. Ruas, Z. Pan, X. Cheng, A. Arredouani, X. Hao, J. Tang, K. Rietdorf, L. Teboul, K.T. Chuang, et al. 2009. NAADP mobilizes calcium from acidic organelles through two-pore channels. *Nature.* 459:596–600.

Cancela, J.M., G.C. Churchill, and A. Galione. 1999. Coordination of agonist-induced Ca^{2+}-signalling patterns by NAADP in pancreatic acinar cells. *Nature.* 398:74–76.

Churchill, G.C., Y. Okada, J.M. Thomas, A.A. Genazzani, S. Patel, and A. Galione. 2002. NAADP mobilizes Ca^{2+} from reserve granules, lysosome-related organelles, in sea urchin eggs. *Cell.* 111:703–708.

Churchill, G.C., J.S. O`Neil, R. Masgrau, S. Patel, J.M. Thomas, A.A. Genazzani, and A. Galione. 2003. Sperm deliver a new messenger:NAADP. *Curr. Biol.* 13:125–128.

Copello, J.A., Y. Qi, L.H. Jeyakumar, E. Ogunbunmi, and S. Fleischer. 2001. Lack of effect of cADP-ribose and NAADP on the activity of skeletal muscle and heart ryanodine receptors. *Cell Calcium.* 30:269–284.

Dong, X.P., X. Cheng, E. Mills, M. Delling, F. Wang, T. Kurz, and H. Xu. 2008. The type IV mucolipidosis-associated protein TRPML1 is an endolysosomal iron release channel. *Nature.* 455:992–996.

Fill, M., and J.A. Copello. 2002. Ryanodine receptor calcium release channels. *Physiol. Rev.* 82:893–922.

Foskett, J.K., C. White, K.H. Cheung, and D.O. Mak. 2007. Inositol trisphosphate receptor Ca2+ release channels. *Physiol. Rev.* 87:593–658.

Galione, A., and O.H. Petersen. 2005. The NAADP receptor: new receptors or new regulation? *Mol. Interv.* 5:73–79.

Gambara, G., R.A. Billington, M. Debidda, A. D'Alessio, F. Palombi, E. Ziparo, A.A. Genazzani, and A. Filippini. 2008. NAADP-induced Ca^{2+} signaling in response to endothelin is via the receptor subtype B and requires the integrity of lipid rafts/caveolae. *J. Cell. Physiol.* 216:396–404.

Gerasimenko, J.V., Y. Maruyama, K. Yano, N. Dolman, A.V. Tepikin, O.H. Petersen, and O.V. Gerasimenko. 2003. NAADP mobilizes Ca^{2+} from a thapsigargin-sensitive store in the nuclear envelope by activating ryanodine receptors. *J. Cell Biol.* 163:271–282.

Guse, A.H., and H.C. Lee. 2008. NAADP: a universal Ca2+ trigger. *Sci. Signal.* 1:re10.

Hohenegger, M., J. Suko, R. Gscheidlinger, H. Drobny, and A. Zidar. 2002. Nicotinic acid-adenine dinucleotide phosphate activates the skeletal muscle ryanodine receptor. *Biochem. J.* 367:423–431.

Horton, R.M., Z.L. Cai, S.N. Ho, and L.R. Pease. 1990. Gene splicing by overlap extension: tailor-made genes using the polymerase chain reaction. *Biotechniques.* 8:528–535.

Ishibashi, K., M. Suzuki, and M. Imai. 2000. Molecular cloning of a novel form (two-repeat) protein related to voltage-gated sodium and calcium channels. *Biochem. Biophys. Res. Commun.* 270:370–376.

Kim, B.J., K.H. Park, C.Y. Yim, S. Takasawa, H. Okamoto, M.J. Im, and U.H. Kim. 2008. Generation of nicotinic acid adenine dinucleotide phosphate and cyclic ADP-ribose by glucagon-like peptide-1 evokes Ca2+ signal that is essential for insulin secretion in mouse pancreatic islets. *Diabetes.* 57:868–878.

Kinnear, N.P., F.X. Boittin, J.M. Thomas, A. Galione, and A.M. Evans. 2004. Lysosome-sarcoplasmic reticulum junctions: a trigger zone for calcium signalling by NAADP and endothelin-1. *J. Biol. Chem.* 279(52):54319–54326.

Lee, H.C. 2005. NAADP-mediated calcium signaling. *J. Biol. Chem.* 280(40):33693–33696.

Lee, H.C., and R. Aarhus. 1995. A derivative of NADP mobilizes calcium stores insensitive to inositol trisphosphate and cyclic ADP-ribose. *J. Biol. Chem.* 270:2152–2157.

Marchant, J.S., and I. Parker. 2001. *Xenopus tropicalis* oocytes as an advantageous model system for the study of intracellular Ca(2+) signalling. *Br. J. Pharmacol.* 132:1396–1410.

Masgrau, R., G.C. Churchill, A.J. Morgan, S.J.H. Ashcroft, and A. Galione. 2003. NAADP: a new second messenger for glucose-induced Ca^{2+} responses in clonal pancreatic β-cells. *Curr. Biol.* 13:247–251.

Mitchell, K.J., F.A. Lai, and G.A. Rutter. 2003. Ryanodine receptor type I and nicotinic acid adenine dinucleotide phosphate (NAADP) receptors mediate Ca^{2+} release from insulin-containing vesicles in living pancreatic β cells (MIN6). *J. Biol. Chem.* 278:11057–11064.

Mojzisova, A., O. Krizanova, L. Zacikova, V. Kominkova, and K. Ondrias. 2001. Effect of nicotinic acid adenine dinucleotide phosphate on ryanodine calcium release channel in heart. *Pflugers. Arch.* 441:674–677.

Naylor, E., A. Arredouani, S.R. Vasudevan, A.M. Lewis, R. Parkesh, A. Mizote, D. Rosen, J.M. Thomas, M. Izumi, A. Ganesan, et al. 2009. Identification of a chemical probe for NAADP by virtual screening. *Nat. Chem. Biol.* 5:220–226.

Patel, S., G.C. Churchill, and A. Galione. 2001. Coordination of Ca^{2+} signalling by NAADP. *Trends Biochem. Sci.* 26:482–489.

Peiter, E., F.J. Maathuis, L.N. Mills, H. Knight, J. Pelloux, A.M. Hetherington, and D. Sanders. 2005. The vacuolar Ca2+-activated channel TPC1 regulates germination and stomatal movement. *Nature.* 434:404–408.

Pottosin, I.I., and G. Schonknecht. 2007. Vacuolar calcium channels. *J. Exp. Bot.* 58:1559–1569.

Schrlau, M.G., E. Brailoiu, S. Patel, Y. Gogotsi, N.J. Dun, and H.M. Bau. 2008. Carbon nanopipettes characterize calcium release pathways in breast cancer cells. *Nanotechnology.* 19:325102.

Sherer, N.M., M.J. Lehmann, L.F. Jimenez-Soto, A. Ingmundson, S.M. Horner, G. Cicchetti, P.G. Allen, M. Pypaert, J.M. Cunningham, and W. Mothes.

Downloaded from http://rupress.org/jcb/article-pdf/186/2/201/1892586/jcb_200904073.pdf by guest on 08 February 2026

2003. Visualization of retroviral replication in living cells reveals budding into multivesicular bodies. *Traffic.* 4:785–801.

Steen, M., T. Kirchberger, and A.H. Guse. 2007. NAADP mobilizes calcium from the endoplasmic reticular Ca(2+) store in T-lymphocytes. *J. Biol. Chem.* 282:18864–18871.

Subramanian, V.S., J.S. Marchant, I. Parker, and H.M. Said. 2001. Intracellular trafficking/membrane targeting of human reduced folate carrier expressed in *Xenopus* oocytes. *Am. J. Physiol. Gastrointest. Liver Physiol.* 281:G1477–G1486.

Sulem, P., D.F. Gudbjartsson, S.N. Stacey, A. Helgason, T. Rafnar, M. Jakobsdottir, S. Steinberg, S.A. Gudjonsson, A. Palsson, G. Thorleifsson, et al. 2008. Two newly identified genetic determinants of pigmentation in Europeans. *Nat. Genet.* 40:835–837.

Yamasaki, M., R. Masgrau, A.J. Morgan, G.C. Churchill, S. Patel, S.J.H. Ashcroft, and A. Galione. 2004. Organelle selection determines agonist-specific Ca^{2+} signals in pancreatic acinar and beta cells. *J. Biol. Chem.* 279:7234–7240.

Zhang, F., and P.L. Li. 2007. Reconstitution and characterization of a nicotinic acid adenine dinucleotide phosphate (NAADP)-sensitive Ca2+ release channel from liver lysosomes of rats. *J. Biol. Chem.* 282:25259–25269.

Zhang, F., G. Zhang, A.Y. Zhang, M.J. Koeberl, E. Wallander, and P.L. Li. 2006. Production of NAADP and its role in Ca2+ mobilization associated with lysosomes in coronary arterial myocytes. *Am. J. Physiol. Heart Circ. Physiol.* 291:H274–H282.

Downloaded from http://rupress.org/jcb/article-pdf/186/2/201/1892586/jcb_200904073.pdf by guest on 08 February 2026